ELSEVIER

The apical disposition of the *Caenorhabditis elegans* intestinal terminal web is maintained by LET-413 [☆]

Olaf Bossinger,[a,]* Tetsunari Fukushige,[b,1] Myriam Claeys,[c]
Gaetan Borgonie,[c] and James D. McGhee[b,]*

[a]*Institut für Genetik, Heinrich-Heine-Universität Düsseldorf, D-40225 Düsseldorf, Germany*
[b]*Genes and Development Research Group, Department of Biochemistry and Molecular Biology, University of Calgary, Calgary, Alberta, Canada T2N 4N1*
[c]*Department of Biology, University Ghent, B-9000 Ghent, Belgium*

Abstract

We wish to understand how organ-specific structures assemble during embryonic development. In the present paper, we consider what determines the subapical position of the terminal web in the intestinal cells of the nematode *Caenorhabditis elegans*. The terminal web refers to the organelle-depleted, intermediate filament-rich layer of cytoplasm that underlies the apical microvilli of polarized epithelial cells. It is generally regarded as the anchor for actin rootlets protruding from the microvillar cores. We demonstrate that: (i) the widely used monoclonal antibody MH33 reacts (only) with the gut-specific intermediate filament protein encoded by the *ifb-2* gene; (ii) IFB-2 protein accumulates near the gut lumen beginning at the lima bean stage of embryogenesis and remains associated with the gut lumen into adulthood; and (iii) as revealed by immunoelectron microscopy, IFB-2 protein is confined to a discrete circumferential subapical layer within the intestinal terminal web (known in nematodes as the "endotube"); this layer joins directly to the apical junction complexes that connect adjacent gut cells. To investigate what determines the disposition of the IFB-2-containing structure as the terminal web assembles during development, RNAi was used to remove the functions of gene products previously shown to be involved in the overall apicobasal polarity of the developing gut cell. Removal of *dlg-1*, *ajm-1*, or *hmp-1* function has little effect on the overall position or continuity of the terminal web IFB-2-containing layer. In contrast, removal of the function of the *let-413* gene leads to a basolateral expansion of the terminal web, to the point where it can now extend around the entire circumference of the gut cell. The same treatment also leads to concordant basolateral expansion of both gut cell cortical actin and the actin-associated protein ERM-1. LET-413 has previously been shown to be basolaterally located and to prevent the basolateral expansion of several individual apical proteins. In the present context, we conclude that LET-413 is also necessary to maintain the entire terminal web or brush border assembly at the apical surface of *C. elegans* gut cells, a dramatic example of the so-called "fence" function ascribed to epithelial cell junctions. On the other hand, LET-413 is not necessary to establish this apical location during early development. Finally, the distance at which the terminal web intermediate filament layer lies beneath the gut cell surface (both apical and basolateral) must be determined independently of apical junction position.
© 2004 Elsevier Inc. All rights reserved.

Keywords: Caenorhabditis elegans; Intestine; Epithelium; Terminal web; Intermediate filament; IFB-2; MH33; Apical–basal polarity; Intercellular junctions

Introduction

Organ formation during development often involves the assembly of complex cellular structures intimately connected with organ function. A striking example of such a structure is provided by the microvillar brush border surrounding the lumen of metazoon intestines. We wish to investigate the molecular mechanisms that establish such organ-specific structures during development and are focusing on organogenesis of the *Caenorhabditis elegans* intestine. In the present paper, we investigate the formation of the

so-called "terminal web," an elaborate but incompletely defined subapical structure generally believed to function as an anchor for the actin bundles protruding from the overlying brush border microvilli.

The intestinal terminal web has been investigated at the ultrastructural level (Hirokawa et al., 1982) and the principal components are known to be intermediate filaments, myosin, spectrin, and an assortment of actin-binding proteins (see reviews in Fath and Burgess, 1995; Ku et al., 1999; Mooseker, 1985; Thomas, 2001). Terminal web assembly has been described during gut development in vertebrates (Chambers and Grey, 1979), but the molecular details of the assembly process are largely unexplored. Furthermore, it is not known how similar the C. elegans intestinal terminal web is to its vertebrate counterpart. As one potentially significant difference, the intestinal terminal web in many nematodes contains a discrete and prominent substructure termed the "endotube" (Munn and Greenwood, 1984; see Fig. 1).

There must be some interplay between the mechanisms that establish and maintain the fundamental apical–basal polarity of intestinal epithelial cells and mechanisms that position the terminal web just beneath the intestinal apical surface. This interplay will be especially interesting to investigate in the C. elegans intestine, where the establishment of apical–basal polarity is being intensely investigated (Asano et al., 2003; Bossinger et al., 2001; Costa et al., 1998; Firestein and Rongo, 2001; Köppen et al., 2001; Legouis et al., 2000, 2003; Leung et al., 1999; McMahon et al., 2001) and where both molecular and functional parallels are being discovered between the single electron-

dense structure of the C. elegans apical junction (CeAJ) and the more complex junctional structures found in Drosophila and vertebrates (see reviews in Knust and Bossinger, 2002; Michaux et al., 2001; Tepass et al., 2001; Tsukita et al., 2001).

Material and methods

C. elegans strains and culture

Standard procedures for handling and maintaining C. elegans have been previously described (Brenner, 1974). Bristol strain N2 was used as wild type. The transgenic strain expressing an actin-5::YFP reporter fusion under control of the gut-specific ges-1 promoter will be described elsewhere (TF, in preparation).

Molecular analysis of ifb-2

Expression screening of a C. elegans cDNA library (kindly provided by Dr. R. Barstead, University of Oklahoma), identification, and characterization of clones and other recombinant DNA manipulations were conducted by standard methods (Sambrook and Russell, 2001).

RNA-mediated interference

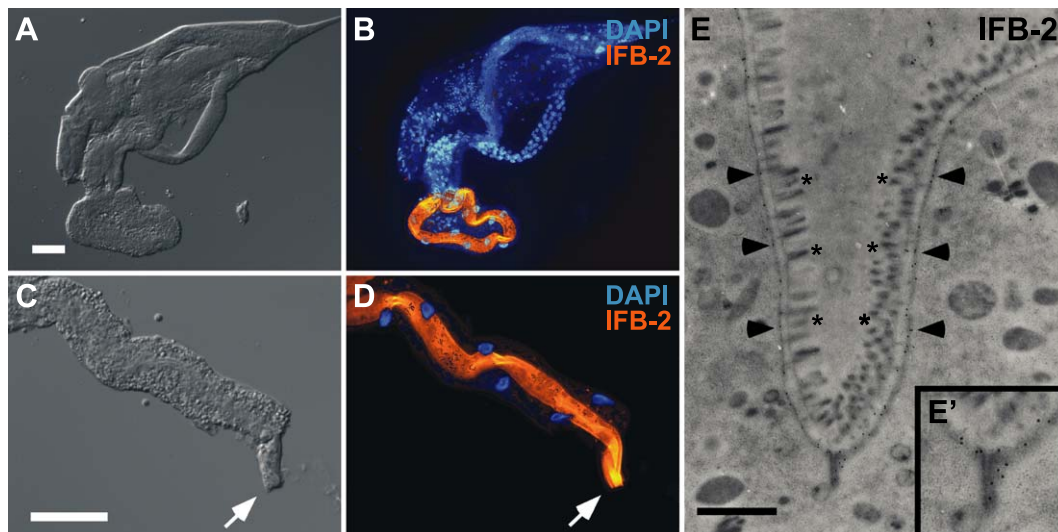The following cDNA clones were obtained from Y. Kohara (Gene Network Lab, NIG, Mishima 411, Japan):

Fig. 1. The monoclonal antibody MH33, which recognizes the IFB-2 intermediate filament protein, reacts specifically with the C. elegans intestine. (A–D) A squashed adult worm (A and B) and an isolated adult intestine (C and D) were either viewed with Nomarski DIC optics (A and C) or stained with DAPI and MH33 (B and D) to visualize nuclei and the intermediate filament IFB-2, respectively. MH33 reactivity is completely restricted to the intestine (B) and stains the so-called "endotube," a tubular structure surrounding the intestinal lumen (C and D, arrow). (E) Immunoelectron micrograph (transverse section) of an adult intestine shows that MH33 (immunogold labeling) reacts with a discrete structure (arrowheads) that encircles the gut lumen and that lies immediately beneath the microvillar brush border (asterisks). (E′) A higher magnification illustrates that the IFB-2 containing structure within the terminal web joins directly into the electron dense structure defining the C. elegans apical junction. (A and C) Nomarski DIC optics, (B and D) immunofluorescence. Scale bars in A, C, and E are 50 μm, 50 μm, and 500 nm, respectively.

for *ajm-1*, yk445g1 (2.6 kB) and yk531e7 (4.3 kB); for *dlg-1*, yk25e5 (2.6 kB) and yk128b7 (2.4 kB); for *hmp-1*, yk271a9 (3.3 kB) and yk675e4 (3.3 kB); and for *let-413*, yk126a10 (2.6 kB) and yk524b7 (3.1 kB). The 5′ and 3′ sequences are specific to the genes being tested, as determined by BLAST searches (http://www.wormbase.org/). Phagemid DNA was prepared as described in the Stratagene ExAssist protocol. Sense and antisense strands of RNA were synthesized using the RiboMAX large-scale RNA in vitro transcription kit (Promega, Inc.) and annealed before injection at 0.5 mg/ml (Fire et al., 1998). The quality of RNAs was checked on a formaldehyde containing 1.8% agarose gel. Microinjections into the gonads of hermaphrodites were observed with Nomarski optics using a Leica DM IRBE inverted microscope equipped with a 40× PL Fluotar objective (NA 1.3). In general, one syncytial gonad of each of 15–20 young adult hermaphrodites was injected, and individual worms were placed on separate seeded plates 18–20 h after injection. Embryos produced by the injected worms were collected 2–8 h after egg laying and prepared for immunostaining as described below.

Immunostaining, microscopy, and image processing

Embryos were isolated by cutting adult worms with a scalpel and subsequently transferred using a drawn-out pipette to a microscope slide coated with a thin layer of polylysine in a drop of distilled water. Embryos were permeabilized by using the freeze–crack method (Strome and Wood, 1983) and fixed in 100% ice-cold methanol (10 min), ice-cold 100% acetone (20 min), ice-cold 90% ethanol (10 min), ice-cold 60% ethanol (10 min), and 30% ethanol (10 min at room temperature). Slides were washed twice for 10 min in TBT (20 mM Tris–HCl; 150 mM NaCl, pH 8.0 + 0.1% Tween 20), incubated at 4°C overnight with primary antibodies (see below) in blocking buffer (TBT plus 1% BSA and 1% nonfat dry milk powder), washed three times for 10 min each with TBT at room temperature, and finally incubated at room temperature for 1–3 h, with secondary antibodies (see below) in blocking buffer. Finally, slides were washed three times for 10 min each in TBT and mounted in Mowiol containing DABCO (1,4-diazabicyclo(2.2.2)octane; Sigma, Inc.) as an antifade reagent. To investigate MH33 staining in the adult gut, young healthy hermaphrodites were collected, washed in water, and cut randomly using a 27-gauge needle. Carcasses were transferred with a capillary into a well slide containing the paraformaldehyde–glutaraldehyde fixative solution used for *ges-1* staining (Edgar and McGhee, 1986) but diluted with an equal volume of distilled water, incubated overnight at 4°C, transferred to a subbed microscope slide, and then processed by freeze cracking as described above for embryos.

The following primary and secondary antibodies were used at the dilutions (in blocking buffer) indicated: anti-IFB-2 (mabMH33, mouse, hybridoma supernatant diluted 1:100), anti-AJM-1 (mabMH27, mouse, hybridoma supernatant, 1:1500), anti-DLG-1 (rabbit, 1:400), anti-PY (rabbit, Biotrend, Inc., 1:100), anti-ERM-1 (rabbit, 1:150), and either Cy2-conjugated or Cy3-conjugated secondary antibodies (1:200, Jackson ImmunoResearch Laboratories).

In the case of double staining of FITC/Alexa Fluor 488-phalloidin and antibodies, embryos were permeabilized by the freeze–crack method (see above), incubated at −20°C for 30 min in a phalloidin/fixative mixture [FITC-phalloidin (Sigma, Inc.) or Alexa Fluor 488-phalloidin (Molecular Probes, Inc.) stock solution (1 mg/ml in PBS) diluted 1:100 in 75% methanol and 3.7% paraformaldehyde], washed twice for 10 min each in PBT (PBS plus 0.1% Tween 20), incubated at RT for 1 h with FITC/Alexa Fluor 488-phalloidin (1:100) in a moist chamber, and washed twice for 10 min each in PBT. Subsequent antibody staining procedures (starting with the incubation of primary antibodies) were carried out as described above. In the case of FITC/Alexa Fluor 488-phalloidin single staining (Costa et al., 1998), embryos were fixed for 2 min in 4% paraformaldehyde in 60 mM Pipes, 25 mM HEPES, 10 mM EGTA, 2 mM MgCl$_2$, pH 6.8 containing 0.1 mg/ml L-α-lysolecithin (Sigma, Inc.), incubated for an additional 20 min in the same fixative but without lysolecithin, washed twice for 10 min each in PBT, and incubated for at least 1 h with FITC/Alexa Fluor 488-phalloidin (1:100).

Immunofluorescence analysis of embryos was performed on a confocal laser-scanning microscope (TCS-NT, Leica, Vienna, Austria) equipped with a 100× PL Fluotar oil-immersion objective. Recorded images represent a Z-projection of optical sections taken 0.5 μm apart. The different stages of morphogenesis were classified by the apparent shape and elongation of the embryo: lima bean (epiboly), comma (end of epiboly), tadpole (1.5-fold), plum (1.75-fold), loop (twofold), and pretzel (fourfold). Final image layout with a resolution of 300–600 dpi was performed on a Dual 2 GHz PowerPC G5 (Apple Computer, Inc.) using Adobe Photoshop 7.0.1 (Adobe Systems, Inc.) and Canvas 9.0.1 (ACD Systems, Inc.) software.

Immunoelectron microscopy

Nematodes were collected in small copper tubes and fixed using the EMPACT high pressure freezing equipment (Leica). Frozen nematodes were subsequently substituted using methanol as sole substitution agent in AFS equipment (Leica). Safranin O (Sigma, Inc.) was added to the water-free methanol solution to slightly color the nematode tissue. Although safranin O is water-soluble, it dissolves to a small extent in methanol. Substitution was carried out using the following slopes or plateaus: (1) 76 h at −85°C followed by a slope of 18.3 h with temperature increase of 3°C/h, (2) a 4-h plateau at −30°C followed by an upwards slope of 17.3 h with 3°C increase each hour to a stable plateau of 4°C. The safranin O was added from the beginning of substitution and removed after slope 2. Impregnation occurred at 4°C with continuous rotation of the samples in LR White

(Laborimpex, Brussels, Belgium) using the following series: methanol/LR white 3:1 for 24 h, methanol/LR white 1:1 for 24 h, methanol/LR white 1:3 for 24 h, and LR white pure refreshed three times in the course of 36 h. Polymerization occurred in gelatin capsules under UV at 4°C for 48 h. After polymerization, the capsules were placed at 60°C for several hours to achieve complete polymerization. Seventy nanometer thick ultrathin sections were prepared using the Ultracut S (Leica) and collected on nickel single slot grids (Laborimpex) covered with a formvar film. Immunohistochemistry using mabMH33 (anti-IFB-2, see above) was carried out by washing the grids 3 × 15 min in phosphate-buffered saline (PBS). The grids were incubated for 2 h at room temperature in undiluted primary mabMH33. Grids were washed 5 × 5 min in PBS followed by incubation in 1:50 diluted 15 nm gold probe goat antimouse IgG (Fc) (Amersham Pharmacia Biotech, Inc.) for 30 min at room temperature. Grids were washed 5 × 5 min in PBS followed by a brief wash in distilled water. Sections were ultrastained using uranylacetate and lead citrate (EM stain, Leica). Sections were analyzed and photographed using a JEOL TEM 1010 operating at 60 kV. Photographs were taken on Kodak electron image film (Estar Thick Base; SO-136) and printed using Brovira Speed (glossy grade normal BN310 RC Nr 3 and Nr 4, Agfa, Inc.) using AgeFix (Agfa, Inc.) as fixative and Neutol Liquid WA (Agfa, Inc.) as developer.

Results and discussion

Identification of IFB-2 as an intestinal terminal web-specific intermediate filament protein

To investigate the developmental assembly of the C. elegans terminal web, it would be a considerable asset to have a specific marker defined at both the molecular and ultrastructural level. Francis and Waterston (1985) produced a series of highly useful monoclonal antibodies using as antigens a crude insoluble fraction produced from mixed stage C. elegans; they noted that one particular member of their monoclonal series, MH33, reacted with the worm intestine. MH33 reactivity has subsequently been used as a marker for early intestine differentiation (see for example, Fukushige et al., 1998; Zhu et al., 1998), and the gene encoding the MH33 epitope is a candidate for a direct downstream target of the C. elegans endodermal GATA factor ELT-2 (Fukushige et al., 1998; Hawkins and McGhee, 1995).

Figs. 1A and B demonstrate that MH33 reactivity in the adult worm is completely restricted to the central region of the intestine, apparently surrounding the intestinal lumen. This is seen more clearly with the isolated adult intestine shown in Figs. 1C and D: MH33 reacts with a tubular structure (arrows in Figs. 1C and D) that can often be seen protruding from the cut end of a dissected intestine where

the gut cell cytoplasm has apparently dissociated. This structure presumably corresponds to the "endotube" described in the intestines of many larger nematodes (Munn and Greenwood, 1984). Immunoelectron microscopy (Fig. 1E) shows that MH33 reacts exclusively with a discrete circumferential layer within the terminal web, closely underlying the intestinal microvillar brush border. As shown in the inset to Fig. 1E, the MH33 reactive layer continues directly into the electron dense regions that define the CeAJ and that join adjacent gut cells.

Weber et al. have identified the entire collection of C. elegans intermediate filament encoding genes, initially on the basis of cross hybridization and subsequently by analysis of the genomic sequence (Dodemont et al., 1994; Karabinos et al., 2001, 2002, 2003). They showed that one particular intermediate filament protein (IFB-2) produced in Escherichia coli reacted with MH33 on Western blots (Karabinos et al., 2001). To determine if MH33 reacted with any other worm protein, we screened approximately 100,000 plaques from a C. elegans mixed stage expression library (Barstead and Waterston, 1989); cross hybridization showed that all 18 purified positive clones corresponded to the same gene; sequencing unambiguously identified the gene as *ifb-2* (F10C1.7). Several further observations unambiguously demonstrate that IFB-2 is the only MH33-reactive epitope in C. elegans: (i) MH33 detects approximately 60–62 kD doublet on Western blots of whole worm extracts (Francis and Waterston, 1985; Karabinos et al., 2001, our unpublished results), and the intensity of both bands is greatly increased in worms transgenic for the *ifb-2* gene (our unpublished results); the *ifb-2* gene is predicted to be alternatively spliced and to encode two proteins of size 59.8 and 61.6 kD (http://www.wormbase.org/); (ii) transgenic reporter constructs (in which approximately 5 kb of 5′-flanking sequence + 21 bps of the predicted *ifb-2* coding region are fused to GFP/*lacZ*) express in a completely gut-specific pattern from embryos to adults (data not shown); and (iii) as will be shown in a later section, RNA-mediated interference using double-stranded RNA produced from the *ifb-2* gene removes all MH33 reactivity from C. elegans embryos and larvae.

Expression of ifb-2 and establishment of the intestinal terminal web during embryonic development

The next step was to determine at what point during embryonic development IFB-2 adopts its subapical location and to define the location of IFB-2 relative to immunofluorescent markers of gut cell apical–basal polarity. Wild-type C. elegans embryos were collected at various stages and stained with both MH33 and with a rabbit polyclonal antibody to the MAGUK protein DLG-1 (Segbert et al., 2004), which has previously been shown to be located in the CeAJ of embryonic epithelial cells (Bossinger et al., 2001; Firestein and Rongo, 2001; Köppen et al., 2001; McMahon et al., 2001; Segbert et al., 2004). Fig. 2A shows a lima bean
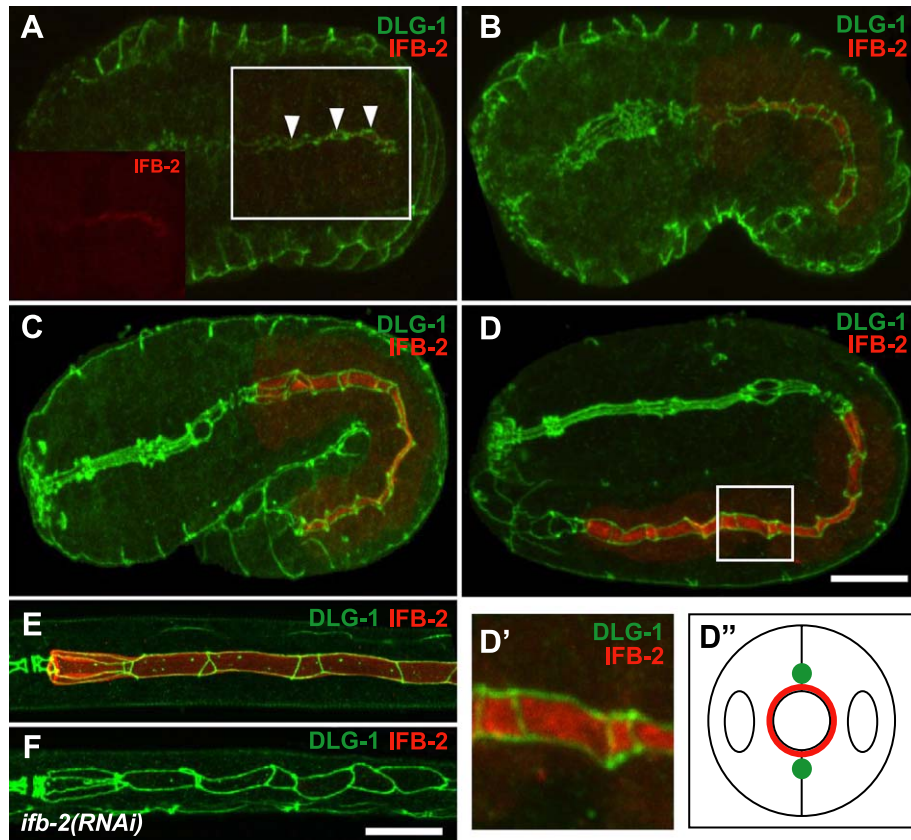
Fig. 2. Expression pattern of the intermediate filament protein IFB-2 and the MAGUK protein DLG-1 during development of the *C. elegans* intestine. (A–D) Immunofluorescence of MH33 (red, anti-IFB-2) and anti-DLG-1 antibodies (green) reveal formation of the intestinal terminal web and the *C. elegans* apical junction (CeAJ), respectively. (A) During early morphogenesis (lima bean stage), a faint MH33 staining becomes visible in the cell cytoplasm, while a fraction of the IFB-2 protein (together with DLG-1) is located in a punctate pattern at the gut midline (arrowheads). (B and C) During ongoing morphogenesis of the intestine (comma stage and plum stage, respectively), cytoplasmic staining of IFB-2 increases and the accumulation near the apical cytocortex becomes more prominent, clearly delineating the future gut lumen. At the same time, the pattern of the CeAJ becomes refined. (D and E) By late morphogenesis (loop stage) and early larval development, the IFB-2 signal has largely disappeared from the cell cytoplasm but is maintained around the gut lumen, within the general borders defined by the CeAJ (see inset, D'). (D'') Schematic cross section of two gut epithelial cells enclosing the common lumen. Colors refer to protein locations defined by the antibody staining shown in D'. Note that IFB-2 surrounds the entire gut lumen, while DLG-1 only forms apical belts joining the paired intestinal cells. (F) RNAi against *ifb-2* completely depletes the IFB-2 protein from the early larval intestine (only anterior part shown) but does not disrupt the pattern of apical junctions. (A–D) Images were taken under identical conditions at the confocal microscope. Orientation: anterior, left; dorsal, top; lateral view. Scale bars in D and F are 10 and 20 μm, respectively.

stage embryo in which IFB-2 can be detected in the gut cell cytoplasm. At this point, gut cells have already established their apical–basal polarity (Leung et al., 1999), and a fraction of the IFB-2 signal can be detected (arrowheads in Fig. 2A) in a faint punctate pattern at the gut midline, the site of the apical membrane domain and the future gut lumen (Leung et al., 1999). As the embryo develops (Figs. 2B and C), the relative amount of IFB-2 staining in the gut cell cytoplasm diminishes until the large majority of IFB-2 is tightly concentrated around the gut lumen (Fig. 2D) within the general boundaries defined by DLG-1 (see inset of Fig. 2D). This location is completely consistent with the location of IFB-2 within the terminal web of the adult intestine, as defined by the immunoelectron microscopy shown above (Fig. 1E). IFB-2 continues to be detected in the intestinal terminal web throughout all later stages examined. Fig. 2E shows an early larval stage that clearly

shows the relative disposition of IFB-2 and DLG-1. Fig. 2F demonstrates that RNAi against the *ifb-2* gene destroys MH33 reactivity in the gut but does not obviously disrupt the intestinal apical junction, nor is there any other obvious phenotype (data not shown, see also Karabinos et al., 2001). However, we cannot rule out a subtle phenotype that might become apparent under other conditions.

Interactions between the intestinal terminal web and genes that establish apical–basal polarity

Double-stranded RNA-mediated interference (RNAi; Fire et al., 1998) provides a convenient and powerful method to determine "what keeps the terminal web terminal," that is, to determine if any of the components involved in *C. elegans* gut cell apical–basal polarity are also involved in the positioning of IFB-2 and the intestinal terminal web.

Fig. 3 collects images of embryos derived from mothers that had been injected with a variety of double-stranded RNAs. Both "early" (approximately 2–4 h after egg laying) and "late" (approximately 6–8 h after egg laying) embryos were then stained with MH33 (to mark the terminal web) and with polyclonal antibodies to either DLG-1 or phosphotyrosine epitopes (to mark the CeAJ of gut cells; Bossinger et al., 2001; Segbert et al., 2004). The embryos shown in Fig. 3 represent RNAi depletion of, roughly speaking, the three separable "systems" associated with the apical junction (Knust and Bossinger, 2002). As can be seen in Figs. 3A and B, depletion of HMP-1 (α-catenin; Costa et al., 1998) or other components of the cadherin–catenin system (data not shown) does not cause a major disruption of the intestinal terminal web. The terminal web contours might be slightly more irregular than wild type (compare to Fig. 2D), but the position remains close to the apical surface [see also online video supplement, Movie 1;
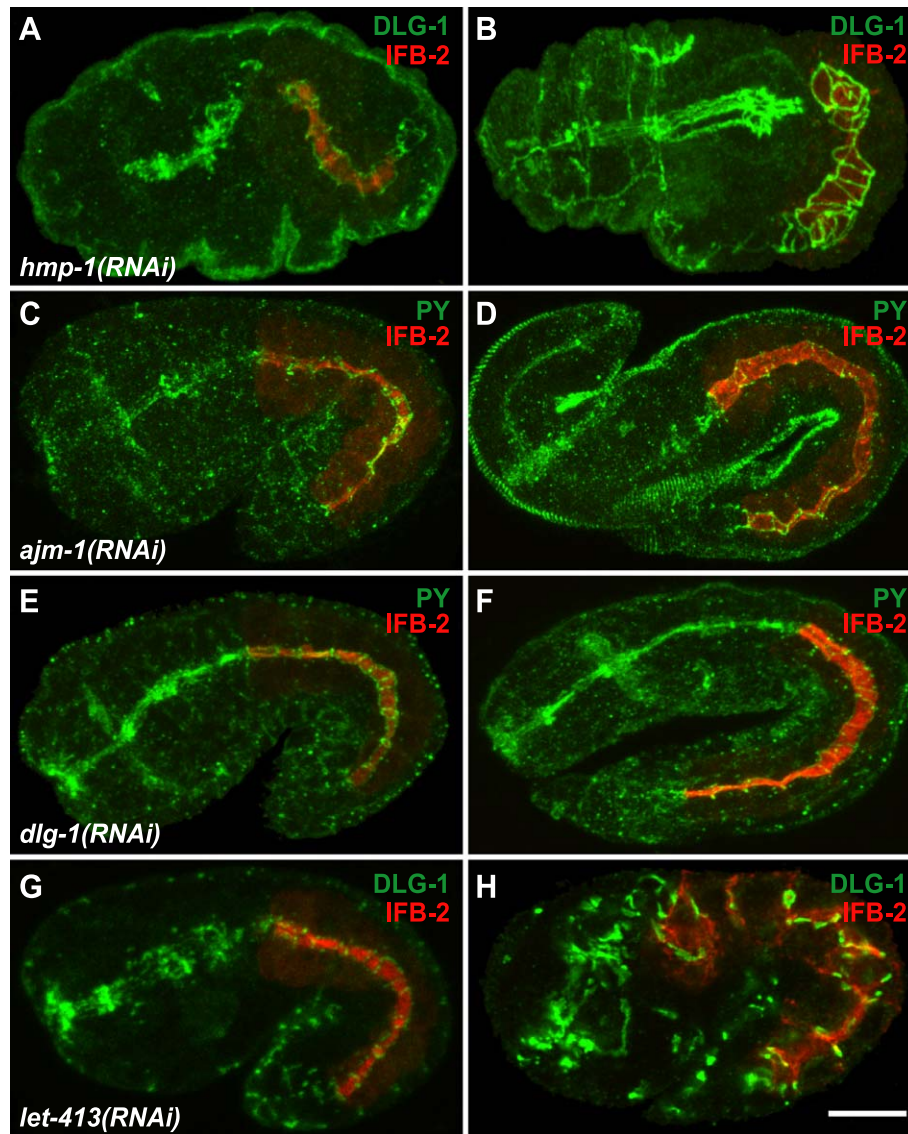

Fig. 3. The role of HMP-1, AJM-1, DLG-1, and LET-413 in maintaining the normal disposition of the intestinal terminal web. Embryos derived from mothers that had been injected with double-stranded RNA against *hmp-1* (α-catenin), *ajm-1* (which encodes a coiled coil protein), *dlg-1* (the homolog of *Drosophila* discs large), and *let-413* (the *Drosophila* scribble homolog) were stained with both MH33 (to recognize the intermediate filament IFB-2 in the terminal web; red) and polyclonal antibodies either against DLG-1 or phosphotyrosine (PY) epitopes (to mark the *C. elegans* apical junction, CeAJ; green). (A, C, E, and G) In embryos (harvested at a time approximately equivalent to the tadpole stage), depletion of HMP-1, AJM-1, DLG-1, or LET-413 neither abolishes nor alters the position of the IFB-2-rich layer in the intestinal terminal web; MH33 staining remains within the boundaries defined by the CeAJ. (B, D, F, and H) In embryos harvested at a time approximately equivalent to the plum or twofold stage, the IFB-2 signal is maintained in the apical cytocortex when HMP-1, AJM-1, and DLG-1 are depleted (B, D and F); while in *let-413*(RNAi) embryos (H), IFB-2 and the terminal web spread along the lateral membrane domains of gut epithelial cells until eventually the whole cell can be ringed with MH33 staining. Orientation: anterior, left; (A–C, E–H) dorsal, top; (A–C, E–H) lateral view. Scale bar: 10 μm.

movies were generated from serial sections of *hmp-1*(RNAi) and *let-413*(RNAi) embryos, respectively]. Figs. 3C and D show that RNAi to *ajm-1* may also cause some roughness in the MH33 staining pattern but, by and large, has little effect on the disposition of either IFB-2 or the phosphotyrosine epitopes with which AJM-1 is tightly associated (Bossinger et al., 2001). Figs. 3E and F show that *dlg-1* RNAi also has little effect on the pattern of IFB-2. All the above results are generally expected based on the relatively minor effect that RNAi against *hmp-1*, *ajm-1*, and *dlg-1* has on the disposition of other apical markers such as PAR-3, PAR-6, and PKC-3 (Bossinger et al., 2001; Köppen et al., 2001; and our unpublished results).

In contrast to the minor effects caused by RNAi depletion of HMP-1, AJM-1, or DLG-1, depletion of LET-413 has a major effect on the disposition of IFB-2 and the terminal web. As can be seen in Figs. 3G and H, *let-413* RNAi embryos show MH33 staining that now extends down the sides of the gut cells until eventually the entire gut cell can be encircled (see also online video supplement, Movie 2). *let-413* encodes the homolog of the *Drosophila* Scribble protein (Bilder and Perrimon, 2000) and is known to be located in the basolateral membrane of both *C. elegans* gut and hypodermal cells (Legouis et al., 2000, 2003; McMahon et al., 2001). Removal of *let-413*

function has been previously shown to allow lateral expansion of normally apical proteins such as PAR-3, PAR-6 (McMahon et al., 2001), and PKC-3 (our unpublished results). The question addressed in the following section is whether the entire brush border or terminal web structure expands, not just individual apical proteins. Comparison of the MH33 staining patterns seen in "early" *let-413*(RNAi) embryos (Fig. 3G) and "late" *let-413*(RNAi) embryos (Fig. 3H) allows us to conclude that this expansion is progressive: IFB-2 spreads along the lateral surfaces of the gut cells but high levels also remain near the original apical surface, although the distribution appears to become more discontinuous in older embryos. Double RNAi to both *let-413* and to *dlg-1* showed roughly the same IFB-2 expansion caused by RNAi to *let-413* by itself (data not shown).

LET-413 also restrains basolateral expansion of other markers of the terminal web or microvillar brush border

Does the entire microvillar brush border structural complex expand along with the intestinal terminal web when *let-413* function is removed? In both wild-type and early *let-413*(RNAi) embryos (approximately lima bean stage), fluorescent phalloidin reveals an accumulation of
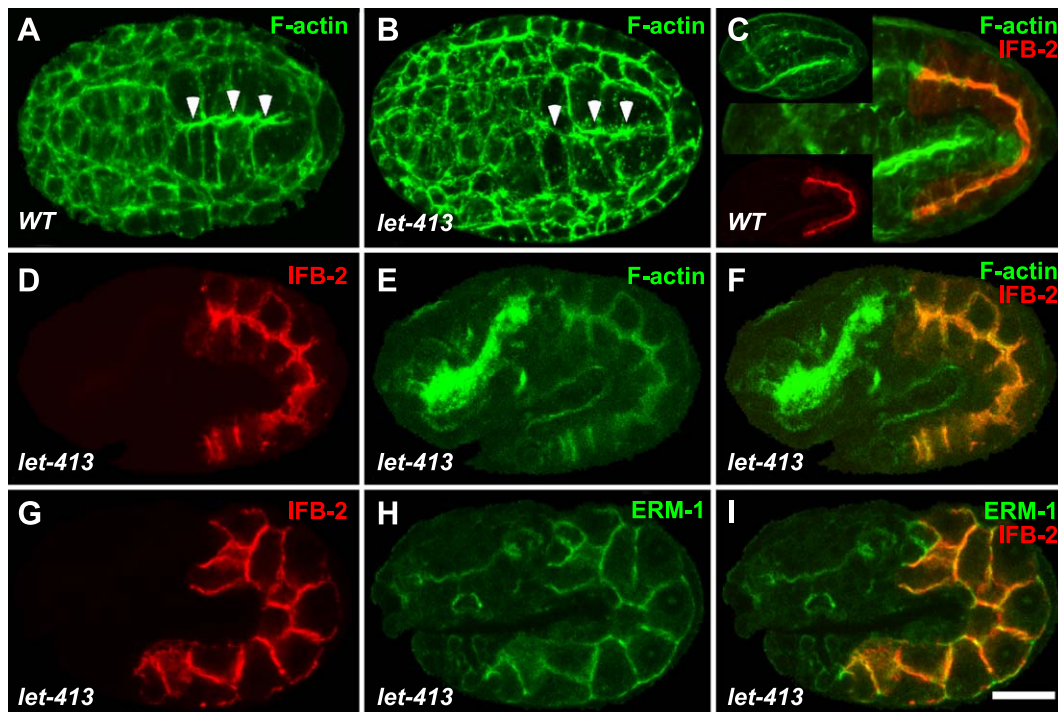

Fig. 4. The actin-rich gut cell cortex and the Ezrin–Radixin–Moesin homolog ERM-1 expand along with the terminal web intermediate filament protein IFB-2 in *let-413*(RNAi) embryos. (A and B) In early morphogenesis (equivalent to lima bean stage), actin filaments (stained with fluorescent phalloidin) accumulate in the apical cytocortex (arrowheads) of both wild-type embryos and *let-413*(RNAi) embryos. (C) In late morphogenesis (equivalent to plum stage), IFB-2, F-actin, and ERM-1 (data not shown) remain apically localized in wild-type embryos. (D–I) However, in *let-413*(RNAi) embryos (harvested at a time approximately equivalent to the plum stage), IFB-2 (D and G), F-actin (E), and ERM-1 (H) expand over the lateral and basal surfaces. The merged images in F and I show that the IFB-2, F-actin, and ERM-1 expansions are largely concordant. Orientation: anterior, left; (A and B) dorsal view; (C–I) dorsal top, lateral view. Scale bar: 10 μm.

F-actin at the apical surface of the gut (Figs. 4A and B, respectively). In older wild-type embryos (plum stage), this F-actin accumulation is maintained and is closely associated with IFB-2 in the terminal web (Fig. 4C). In contrast, in older *let-413*(RNAi) embryos, both MH33 reactivity (Fig. 4D) and fluorescent phalloidin staining (Fig. 4E) expand from the apical onto the basolateral surfaces (see online video supplement, Movies 2 and 3). The merged image in Fig. 4F shows that the F-actin and IFB-2 expansions appear concordant. To support these results, RNAi depletion of *let-413* function was repeated in a transgenic strain of worms in which a chimeric actin-YFP reporter was expressed under control of the gut-specific *ges-1* promoter. Actin-YFP fluorescence in early *let-413*(RNAi) embryos is concentrated at the apical surface of the gut cells (just as in wild-type embryos), but the actin-YFP fluorescence in later *let-413*(RNAi) embryos is seen to expand basolaterally to the point where it ultimately encircles the entire gut cell, just as was seen above with fluorescent phalloidin (data not shown). Figs. 4G–I show the same *let-413*(RNAi)-induced basolateral expansion of the actin-binding protein ERM-1, the *C. elegans* Ezrin–Radixin–Moesin homolog (D. van Fürden and O.B., unpublished results).

The above results suggest that the entire terminal web or microvillar brush border structure expands basolaterally when *let-413* is removed. On the other hand, electron microscopy of sectioned *let-413*(RNAi) embryos does not show actual microvilli extending along the basolateral surfaces, suggesting that under these conditions, the microvillar actin cores either have never developed or have collapsed and are now simply part of the "actin-rich cortex." Finally, we were unable to identify an intestinal lumen in these *let-413*(RNAi) embryos (see also Legouis et al., 2000), probably because *let-413*(RNAi) embryos show an altered morphology of the overall gut; the normal spatial relation between the pair of gut cells within each intestinal ring ("int") is no longer rigidly maintained, and individual gut cells appear free to move and conform to the position of neighboring cells (data not shown).

Summary and conclusions

1. The monoclonal antibody MH33 reacts (only) with an intermediate filament protein, the product of the *C. elegans ifb-2* gene.
2. The IFB-2 intermediate filament protein is located (only) in the subapical terminal web of the *C. elegans* intestine, beginning from the lima bean stage of embryogenesis and continuing into adulthood. IFB-2 reactivity, as detected by immunoelectron microscopy, is confined to the "endotube," a discrete subapical layer surrounding the gut lumen. IFB-2 reactivity continues into the region where the terminal web endotube joins the electron dense structures of the intestinal apical junctions.
3. RNAi depletion of most known components of the intestinal apical junction has little effect on the position or structure of the terminal web. However, removal of *let-413* function allows expansion of the terminal web onto the lateral surfaces and ultimately onto the basal surfaces as well, to the point where the terminal web can now completely encircle the developing gut cell. At the same time, the actin-rich ERM-1-rich cortex also expands from the apical onto the basolateral regions of the gut cells. We suggest that *let-413* prevents the basolateral expansion of the entire brush border or terminal web structure of the *C. elegans* enterocyte.
4. Because the expansion of the terminal web and the actin-rich cortex is progressive, with apical presence being maintained, we conclude that the role of *let-413* is to maintain (not establish) the original apical position of these structures. That is, in the *let-413*(RNAi) embryos, the initial positional cue for apical brush border or terminal web assembly must remain intact, at least in the early embryo.
5. The *let-413* results can rule out a simple model in which the intermediate filament containing layer of the terminal web adopts its position simply by spanning between apical junctions. The observation that in the *let-413* RNAi embryos the terminal web intermediate filament layer remains close to the membrane surface (even basolaterally) would favor a model in which the depth of the intermediate filaments beneath the cell surface is determined by a property of the entire brush border or terminal web assembly. Because normal microvilli are no longer present under the conditions of basolateral expansion, the surface-to-terminal web spacing is unlikely to be imposed by the length of the microvillar rootlets.
6. The results and reagents described in the present paper should provide a starting point from which to investigate the assembly of the entire microvillar brush border or terminal web structural complex during embryonic development of the *C. elegans* intestine.

References

Asano, A., Asano, K., Sasaki, H., Furuse, M., Tsukita, S., 2003. Claudins in *Caenorhabditis elegans*: their distribution and barrier function in the epithelium. Curr. Biol. 13, 1042–1046.

Barstead, R.J., Waterston, R.H., 1989. The basal component of the nematode dense-body is vinculin. J. Biol. Chem. 264, 10177–10185.

Bilder, D., Perrimon, N., 2000. Localization of apical epithelial determinants by the basolateral PDZ protein Scribble. Nature 403, 676–680.

Bossinger, O., Klebes, A., Segbert, C., Theres, C., Knust, E., 2001. Zonula adherens formation in *Caenorhabditis elegans* requires *dlg-1*, the homologue of the *Drosophila* gene discs large. Dev. Biol. 230, 29–42.

Brenner, S., 1974. The genetics of *Caenorhabditis elegans*. Genetics 77, 71–94.

Chambers, C., Grey, R.D., 1979. Development of the structural components of the brush border in absorptive cells of the chick intestine. Cell Tissue Res. 204, 387–405.

Costa, M., Raich, W., Agbunag, C., Leung, B., Hardin, J., Priess, J.R., 1998. A putative catenin–cadherin system mediates morphogenesis of the *Caenorhabditis elegans* embryo. J. Cell Biol. 141, 297–308.

Dodemont, H., Riemer, D., Ledger, N., Weber, K., 1994. Eight genes and alternative RNA processing pathways generate an unexpectedly large diversity of cytoplasmic intermediate filament proteins in the nematode *Caenorhabditis elegans*. EMBO J. 13, 2625–2638.

Edgar, L.G., McGhee, J.D., 1986. Embryonic expression of a gut-specific esterase in *Caenorhabditis elegans*. Dev. Biol. 114, 109–118.

Fath, K.R., Burgess, D.R., 1995. Microvillus assembly. Not actin alone. Curr. Biol. 5, 591–593.

Fire, A., Xu, S., Montgomery, M.K., Kostas, S.A., Driver, S.E., Mello, C.C., 1998. Potent and specific genetic interference by double-stranded RNA in *Caenorhabditis elegans*. Nature 391, 806–811.

Firestein, B.L., Rongo, C., 2001. *DLG-1* is a MAGUK similar to SAP97 and is required for adherens junction formation. Mol. Biol. Cell 12, 3465–3475.

Francis, G.R., Waterston, R.H., 1985. Muscle organization in *Caenorhabditis elegans*: localization of proteins implicated in thin filament attachment and I-band organization. J. Cell Biol. 101, 1532–1549.

Fukushige, T., Hawkins, M.G., McGhee, J.D., 1998. The GATA-factor *elt-2* is essential for formation of the *Caenorhabditis elegans* intestine. Dev. Biol. 198, 286–302.

Hawkins, M.G., McGhee, J.D., 1995. *elt-2*, A second GATA factor from the nematode *Caenorhabditis elegans*. J. Biol. Chem. 270, 14666–14671.

Hirokawa, N., Tilney, L.G., Fujiwara, K., Heuser, J.E., 1982. Organization of actin, myosin, and intermediate filaments in the brush border of intestinal epithelial cells. J. Cell Biol. 94, 425–443.

Karabinos, A., Schmidt, H., Harborth, J., Schnabel, R., Weber, K., 2001. Essential roles for four cytoplasmic intermediate filament proteins in *Caenorhabditis elegans* development. Proc. Natl. Acad. Sci. U. S. A. 98, 7863–7868.

Karabinos, A., Schulze, E., Klisch, T., Wang, J., Weber, K., 2002. Expression profiles of the essential intermediate filament (IF) protein A2 and the IF protein C2 in the nematode *Caenorhabditis elegans*. Mech. Dev. 117, 311–314.

Karabinos, A., Schulze, E., Schunemann, J., Parry, D.A., Weber, K., 2003. In vivo and in vitro evidence that the four essential intermediate filament (IF) proteins A1, A2, A3 and B1 of the nematode *Caenorhabditis elegans* form an obligate heteropolymeric IF system. J. Mol. Biol. 333, 307–319.

Knust, E., Bossinger, O., 2002. Composition and formation of intercellular junctions in epithelial cells. Science 298, 1955–1959.

Köppen, M., Simske, J.S., Sims, P.A., Firestein, B.L., Hall, D.H., Radice, A.D., Rongo, C., Hardin, J.D., 2001. Cooperative regulation of AJM-1 controls junctional integrity in *Caenorhabditis elegans* epithelia. Nat. Cell Biol. 3, 983–991.

Ku, N.O., Zhou, X., Toivola, D.M., Omary, M.B., 1999. The cytoskeleton of digestive epithelia in health and disease. Am. J. Physiol. 277, G1108–G1137.

Legouis, R., Gansmuller, A., Sookhareea, S., Bosher, J.M., Baillie, D.L., Labouesse, M., 2000. LET-413 is a basolateral protein required for the assembly of adherens junctions in *Caenorhabditis elegans*. Nat. Cell Biol. 2, 415–422.

Legouis, R., Jaulin-Bastard, F., Schott, S., Navarro, C., Borg, J.P., Labouesse, M., 2003. Basolateral targeting by leucine-rich repeat domains in epithelial cells. EMBO Rep. 4, 1096–1100.

Leung, B., Hermann, G.J., Priess, J.R., 1999. Organogenesis of the *Caenorhabditis elegans* intestine. Dev. Biol. 216, 114–134.

McMahon, L., Legouis, R., Vonesch, J.L., Labouesse, M., 2001. Assembly of *C. elegans* apical junctions involves positioning and compaction by LET-413 and protein aggregation by the MAGUK protein DLG-1. J. Cell. Sci. 114, 2265–2277.

Michaux, G., Legouis, R., Labouesse, M., 2001. Epithelial biology: lessons from *Caenorhabditis elegans*. Gene 277, 83–100.

Mooseker, M.S., 1985. Organization, chemistry, and assembly of the cytoskeletal apparatus of the intestinal brush border. Annu. Rev. Cell Biol. 1, 209–241.

Munn, E.A., Greenwood, C.A., 1984. The occurrence of submicrovillar endotube (modified terminal web) and associated structures in the intestinal epithelia of nematodes. Philos. Trans. R. Soc. Lond., A 306, 1–18.

Sambrook, J., Russell, D.W., 2001. Molecular Cloning: A Laboratory Manual. Cold Spring Harbor Laboratory Press, Cold Spring Harbor, NY.

Segbert, C., Johnson, K., Theres, C.D.V.F., Bossinger, O., 2004. Molecular and functional analysis of apical junction formation in the gut epithelium of *C. elegans*. Dev. Biol. 266, 17–26.

Strome, S., Wood, W.B., 1983. Generation of asymmetry and segregation of germ-line granules in early *C. elegans* embryos. Cell 35, 15–25.

Tepass, U., Tanentzapf, G., Ward, R., Fehon, R., 2001. Epithelial cell polarity and cell junctions in *Drosophila*. Annu. Rev. Genet. 35, 747–784.

Thomas, G.H., 2001. Spectrin: the ghost in the machine. BioEssays 23, 152–160.

Tsukita, S., Furuse, M., Itoh, M., 2001. Multifunctional strands in tight junctions. Nat. Rev., Mol. Cell Biol. 2, 285–293.

Zhu, J., Fukushige, T., McGhee, J.D., Rothman, J.H., 1998. Reprogramming of early embryonic blastomeres into endodermal progenitors by a *Caenorhabditis elegans* GATA factor. Genes Dev. 12, 3809–3814.